European Radiology
https://doi.org/10.1007/s00330-023-09467-6

European Radiology
ESR EUROPEAN SOCIETY OF RADIOLOGY

EXPERIMENTAL

Improving puncture accuracy in percutaneous CT-guided needle insertion with wireless inertial measurement unit: a phantom study

Chia-Ying Lin[1] · Wen-Ruei Tang[2] · Po-Chang Chiang[1] · Jenn-Jier James Lien[3] · Pei-Yi Tseng[1] · Yi-Sheng Liu[1] · Chao-Chun Chang[2] · Yau-Lin Tseng[2]

Received: 7 November 2022 / Revised: 7 November 2022 / Accepted: 22 January 2023

Abstract

Objectives A novel method applying inertial measurement units (IMUs) was developed to assist CT-guided puncture, which enables real-time displays of planned and actual needle trajectories. The method was compared with freehand and laser protractor–assisted methods.

Methods The phantom study was performed by three operators with 8, 2, and 0 years of experience in CT-guided procedure conducted five consecutive needle placements for three target groups using three methods (freehand, laser protractor–assisted, or IMU-assisted method). The endpoints included mediolateral angle error and caudocranial angle error of the first pass, the procedure time, the total number of needle passes, and the radiation dose.

Results There was a significant difference in the number of needle passes (IMU 1.2 ± 0.42, laser protractor 2.9 ± 1.6, freehand 3.6 ± 2.0 time, $p < 0.001$), the procedure time (IMU 3.0 ± 1.2, laser protractor 6.4 ± 2.9, freehand 6.2 ± 3.1 min, $p < 0.001$), the mediolateral angle error of the first pass (IMU 1.4 ± 1.2, laser protractor 1.6 ± 1.3, freehand 3.7 ± 2.5 degree, $p < 0.001$), the caudocranial angle error of the first pass (IMU 1.2 ± 1.2, laser protractor 5.3 ± 4.7, freehand 3.9 ± 3.1 degree, $p < 0.001$), and the radiation dose (IMU 250.5 ± 74.1, laser protractor 484.6 ± 260.2, freehand 561.4 ± 339.8 mGy-cm, $p < 0.001$) among three CT-guided needle insertion methods.

Conclusion The wireless IMU improves the angle accuracy and speed of CT-guided needle punctures as compared with laser protractor guidance and freehand techniques.

Key Points

- *The IMU-assisted method showed a significant decrease in the number of needle passes (IMU 1.2 ± 0.42, laser protractor 2.9 ± 1.6, freehand 3.6 ± 2.0 time, $p < 0.001$).*
- *The IMU-assisted method showed a significant decrease in the procedure time (IMU 3.0 ± 1.2, laser protractor 6.4 ± 2.9, freehand 6.2 ± 3.1 min, $p < 0.001$).*
- *The IMU-assisted method showed a significant decrease in the mediolateral angle error of the first pass and the caudocranial angle error of the first pass.*

Keywords Needle guidance · Biopsy · Ablation · Interventional radiology · Phantom

✉ Chao-Chun Chang
i5493149@gmail.com

[1] Department of Medical Imaging, National Cheng Kung University Hospital, College of Medicine, National Cheng Kung University, Tainan, Taiwan

[2] Division of Thoracic Surgery, Department of Surgery, National Cheng Kung University Hospital, College of Medicine, National Cheng Kung University, Tainan, Taiwan

[3] Department of Computer Science and Information Engineering, National Cheng Kung University, Tainan, Taiwan

Abbreviations

CT	Computed tomography
DICOM	Digital Imaging and Communications in Medicine
EM	Electromagnetic
EO	Ethylene oxide
GPS	Global positioning system
GUI	Graphical user interface
IMU	Inertial measurement unit

Published online: 24 February 2023

Introduction

Computed tomography (CT)–guided puncture is a widely used clinical technique used for tumor biopsy, tumor ablation therapy, and drainage tube placement. The ability to precisely puncture small targets is important because repeat punctures can increase patient discomfort, procedure-related complications, and radiation exposure [1–4]. Using conventional puncture techniques, translation from a planned needle insertion angle to the actual insertion angle depends on the operator's visuospatial abilities and experience [5]. Sometimes, these procedures are technically challenging in case of a small target size, or the proximity of vulnerable regional anatomy. Some CT scanners facilitate real-time CT fluoroscopy to aid intervention. However, it is not broadly accepted due to the inherent drawback of relatively high radiation exposure to both the operator and the patient [6]. Over the past three decades, a variety of navigational tools have been developed to provide needle guidance, enhance the accuracy of needle insertion and needle tip positioning, reduce the number of needle adjustments, and decrease radiation exposure and procedure time. Current navigational tools for CT guidance includes electromagnetic (EM) navigation [7], optical tracking [8], laser guidance [9, 10], smartphone guidance [11], and laser protractor guidance. In our hospital, a homemade laser protractor was used to assist CT-guided procedures. However, current navigation systems have yet to be widely adopted in real-world practice because of various limitations, including cost, ergonomics, and added procedural time or workflow complexity [4].

Wireless inertial measurement units (IMUs) are electronic devices that measure a body's specific force, angular rate, and sometimes the orientation of the body, using a combination of accelerometers, gyroscopes, and sometimes magnetometers. IMUs are often applied to maneuver aircraft, determine the direction within a global positioning system (GPS), and track the motion within electronics like cell phones. In medicine, IMUs are usually used to track body kinematics [12–14]. IMUs are light and convenient, low-cost navigation devices that allow the puncture to be performed more precisely and at the appropriate angle. Prior studies showed that IMU-assisted implantation of pedicle screws enhanced the performance of a freehand technique in the thoracic and lumbosacral spine [15, 16]. Our study aims to investigate whether the application of wireless IMUs is superior in terms of accuracy and procedure time for CT-guided punctures as compared to freehand and laser protractor guidance methods.

Methods

The experimental schema is described in Fig. 1. Three operators (C.Y.L., an interventional radiologist with 8 years of experience, P.C.C., a radiology resident with 2 years of experience, and W.R.T., a thoracic surgery fellow without experience in CT-guided procedure) performed five consecutive needle placements for target group A, group B, and group C using three different CT guidance methods: (1) IMU-assisted method, (2) laser protractor–assisted method, (3) Freehand method. Targets group A included five targets with mediolateral angles > 30 degrees, caudocranial angles < 10 degrees; targets group B included five targets with caudocranial angles > 30 degrees, mediolateral angles < 10 degrees; and targets group C included five targets with mediolateral angle > 30 degrees, caudocranial

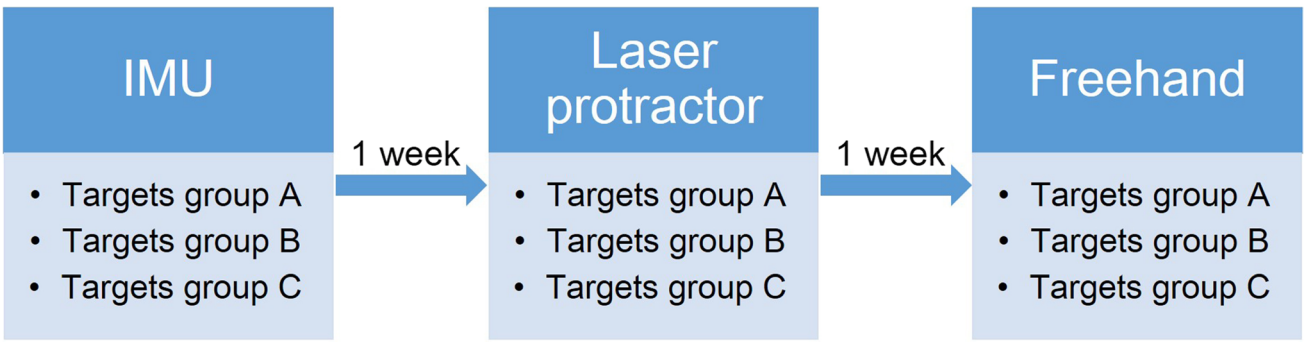

Targets group A = Five targets with mediolateral angle > 30 degrees, caudocranial angles < 10 degrees
Targets group B = Five targets with mediolateral angles < 10 degrees, caudocranial angle > 30 degrees
Targets group C = Five targets with mediolateral angles > 30 degrees, caudocranial angle > 30 degrees

Fig. 1 Experimental flowchart. Three operators performed CT-guided needle insertion for target groups A, B, and C using three methods. The IMU-assisted, laser protractor–assisted, and freehand methods were performed one week apart

Table 1 The detailed information on the target location. In target group A, five targets with large mediolateral angles were used (mediolateral angles > 30 degrees, caudocranial angles < 10 degrees). In target group B, five targets with large caudocranial angles were used (caudocranial angles > 30 degrees, mediolateral angles < 10 degrees). In target group C, five targets with both large mediolateral angles and large caudocranial angles were used (mediolateral angles > 30 degrees, caudocranial angles > 30 degrees)

Target	1st	2nd	3rd	4th	5th
Target group A					
Target depth (cm)	8.9	9.0	9.6	10.8	11.5
Target mediolateral angle (°)	32.9	34.7	40.4	48.1	54.7
Target caudocranial angle (°)	4.9	7.7	9.8	0	9.5
Target group B					
Target depth (cm)	8.9	9.0	9.6	10.8	11.5
Target mediolateral angle (°)	4.9	7.7	9.8	0	9.5
Target caudocranial angle (°)	32.9	34.7	40.4	48.1	54.7
Target group C					
Target depth (cm)	10.5	11.4	10.8	12.5	12.1
Target mediolateral angle (°)	32.1	36.1	40.9	34.6	39.0
Target caudocranial angle (°)	36.2	43.2	34.7	55.1	52.7

angles > 30 degrees (Table 1). The IMU-assisted, laser protractor–assisted, and freehand methods were performed one week apart to avoid the learning effect. The depths of the targets ranged from 8 to 13 cm.

Wireless IMU and hardware

A HI221 HiPNUC wireless IMU, sized 20 × 358.5 mm (W × L × H) and weighed 8.6gm, was used in our study. A laptop with Windows 10 Intel(R) Core(TM) i7-4710MQ @ 2.50 GHz CPU with 16 GB of RAM was used. Our graphical user interface (GUI) integrated the data acquisition from IMU via a wireless USB dongle. The data were stored in real-time on a laptop. The IMU sensors were mounted to the coaxial needle via a self-designed ethylene oxide (EO) gas-sterilized 3D-printed vehicle and covered with a form-fitting sterile, disposable cover (commercial Tegaderm film) (Fig. 2). The output frame rate was 100 Hz. Roll and pitch angle error in the dynamic situation was 2.5 degrees (maximum). The Yaw angle drift was less than 10 degrees in 30 min.

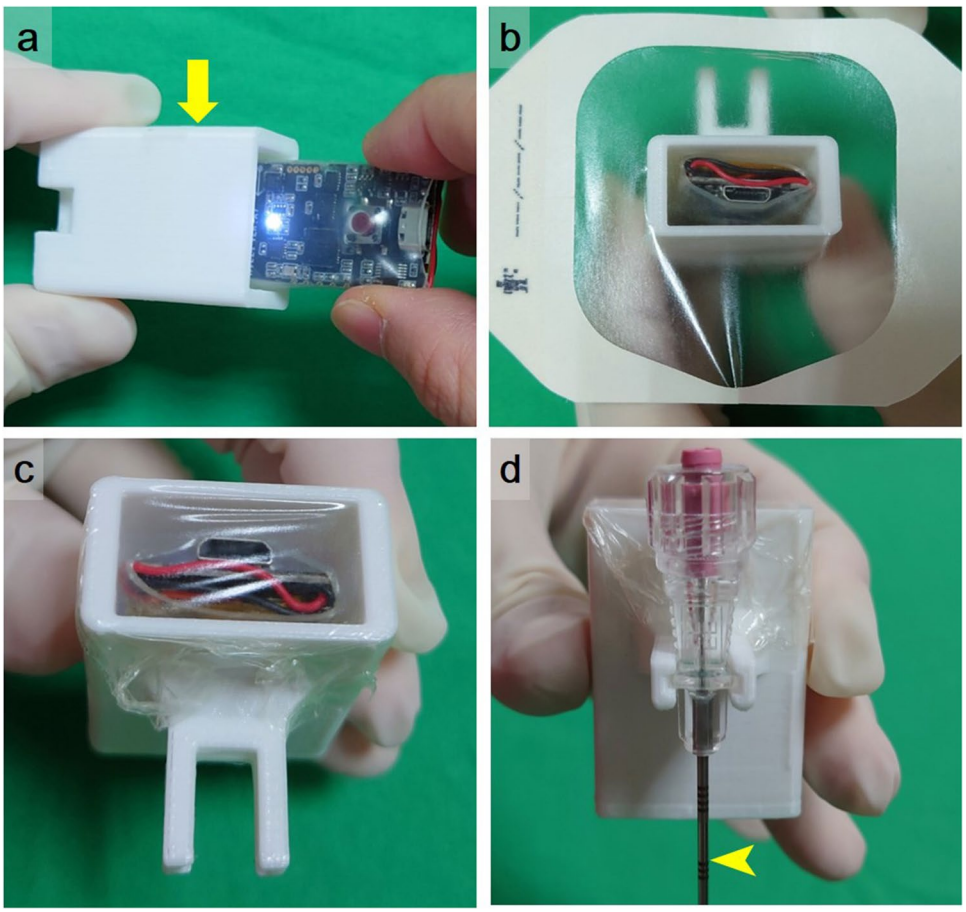

Fig. 2 The IMU setup. **a** IMU sensors were housed in an ethylene oxide (EO) gas sterilized 3D-printed vehicle (arrow). **b**, **c** The 3D-printed vehicle was covered with a form-fitting sterile, disposable cover (commercial Tegaderm film). **d** The 3D-printed vehicle was mounted on the coaxial needle (arrowhead)

Coordinate system and calculations of needle projection angle

Euler angle was extracted with wireless IMU in 6-axis mode (without magnetic calibration). The sensor orientation to its fixed reference system (z-axis parallel and opposite to the gravity vector) was calculated by the IMU software internally. The accelerometer gravity vector contributed to the tilt estimation (roll and pitch), and the gyroscope angular velocity completed the data for the orientation calculation through sensor fusion. Calibration of the IMU was completed by placing the sensor on the CT table parallel to the ground axis to obtain the Euler angle of the CT table (E_0), including row, pitch, yaw (r_0, p_0, y_0) in time $t=0$ (Fig. 3a). Afterwards, IMU was attached to the needle. The angle between the needle and CT table, E_N (row_N, $pitch_N$, yaw_N), was calculated by subtracting the E_t (Euler angle of time $t>0$) by E_{CT}:

$$E_N(r_N,\ p_N,\ y_N) = E_t\ (r_t,\ p_t,\ y_t) - E_{CT}(r_0,\ p_0,\ y_0)$$

After E_N is calculated, it was transferred to the projection angle (Fig. 3b). The needle projection angle on an axial view ($\boldsymbol{\theta a}$) and needle projection angle on a sagittal view ($\boldsymbol{\theta s}$) were obtained using the below formula (Fig. 3c):

$\boldsymbol{ON}$ = needle trajectory length

$\boldsymbol{OA} = \boldsymbol{ON}\cos(p)$

$\boldsymbol{AN} = \boldsymbol{A'N'} = \boldsymbol{A''N''} = \boldsymbol{ON}\sin(p)$

$\boldsymbol{OA'} = \boldsymbol{OA}\sin(y) = \boldsymbol{ON}\cos(p)\sin(y)$

$\boldsymbol{OA''} = \boldsymbol{OA}\cos(y) = \boldsymbol{ON}\cos(p)\cos(y)$

$\boldsymbol{\theta a}$:

$= tan^{-1}(\boldsymbol{A'N'}/\boldsymbol{OA'})$

$= tan^{-1}(\boldsymbol{O}\mathrm{N}\sin(\mathrm{p})/\boldsymbol{O}\mathrm{A}\sin(\mathrm{y}))$

$= tan^{-1}(\boldsymbol{O}\mathrm{N}\sin(\mathrm{p})/\boldsymbol{O}\mathrm{N}\cos(\mathrm{p})\sin(\mathrm{y}))$

$= tan^{-1}(\tan(p)/\sin(y))$

$= tan^{-1}(\tan(p)\csc(\mathrm{y}))$

$\boldsymbol{\theta s}$:

$= tan^{-1}(\boldsymbol{A''N''}/\boldsymbol{OA''})$

$= tan^{-1}(\mathrm{ON}\sin(\mathrm{p})/\mathrm{OA}\cos(\mathrm{y}))$

$= tan^{-1}(\boldsymbol{O}\mathrm{N}\sin(\mathrm{p})/\mathrm{ON}\cos(\mathrm{p})\cos(\mathrm{y}))$

$= tan^{-1}(\tan(p)/\cos(y))$

$= tan^{-1}(\tan(p)\sec(\mathrm{y}))$

where y denotes the yaw angle of the needle; and p denotes the pitch angle of the needle.

Software and systemic framework

A graphical user interface (GUI) was developed with Python (Fig. 4). The Digital Imaging and Communications in Medicine (DICOM) images were transmitted to the processing laptop. The axial view and reformatted sagittal view were shown on the GUI. The entry point and the target were determined by the axial view, and the corresponding angle and length of the trajectories were shown on both axial and sagittal views. Synchronization between the sensors, initial data processing, and coaxial needle calculation was performed. The angle of the IMU was displayed synchronously on the GUI, allowing the operator to adjust the angle in real-time to make it consistent with the planned path.

Experiment setup

The photograph of the experiment setup was demonstrated in Fig. 5. The phantoms in our study were a wet flower mud sponge, sized $22\times10\times7.3$ cm^3 with a 5 mm embedded metallic target bead. The preoperative CT scan was acquired, and the target beads and their associated needle

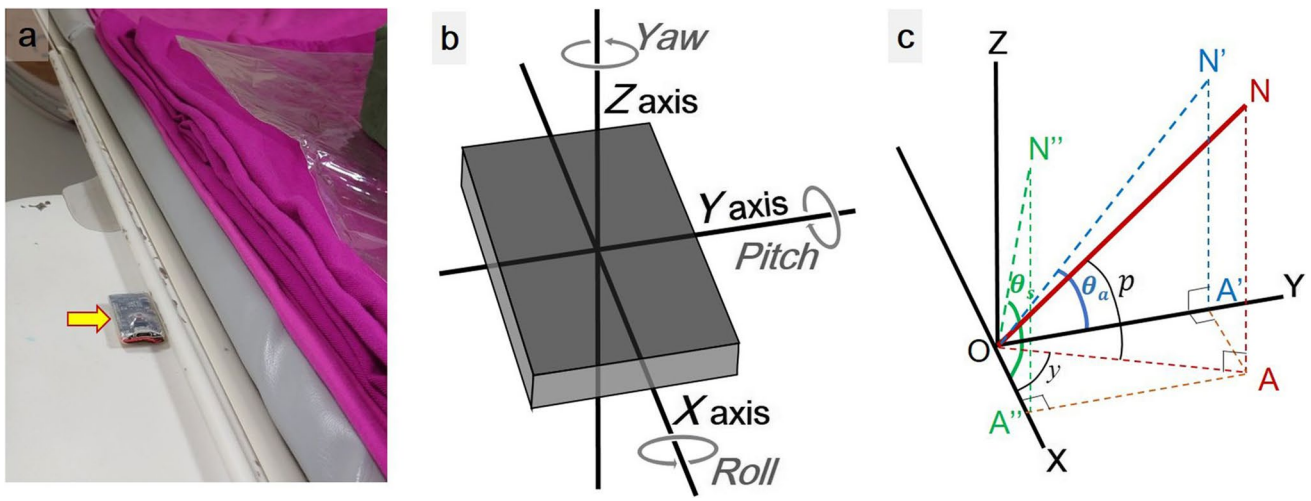

Fig. 3 Calibration of the IMU. **a** Photograph showed calibration of the IMU (arrow) could be done by placing the sensor on the CT table parallel to the ground axis to obtain the Euler angle of the CT table (E_{CT}). **b** Schematic illustration of coordinate frames for IMU. **c** Schematic illustration of converting the Euler angle to projection angle (θa *at YZ* plane and θs at XZ plane)

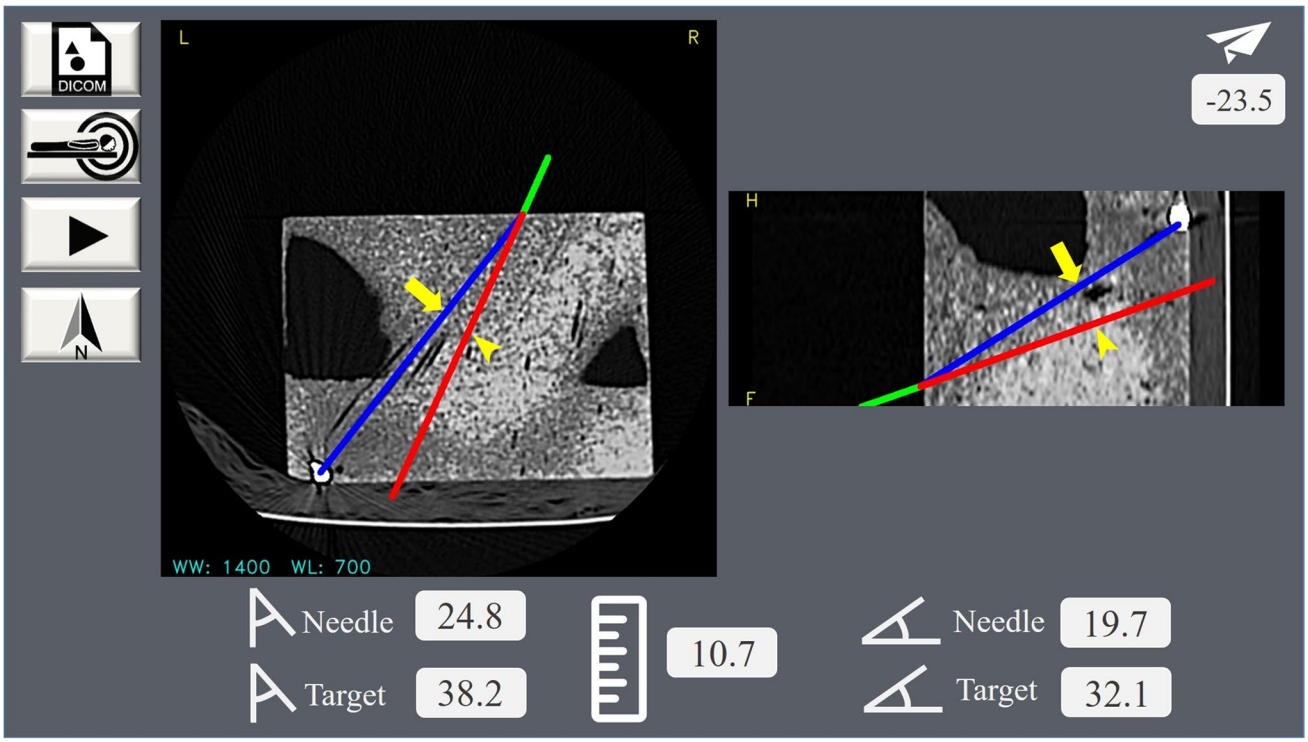

Fig. 4 The screenshot showed graphical user interface (GUI) developed with Python. The DICOM was transmitted to the processing laptop. The entry point and the target were determined on the axial view, and the corresponding angle and length of the desired trajectories (arrow) were displayed on both axial and sagittal views. After synchronization of the sensors and initial data processing, the angle of the IMU (arrowhead) could be displayed on the GUI, allowing real-time angle adjustment

entry points on the surface were defined. A 17-gauge 14.9 cm coaxial needle (Angiotech) was inserted into the wet flower mud sponge. One needle pass was defined as the accomplishment of needle insertion followed by CT confirmation of the location of the biopsy needle tip.

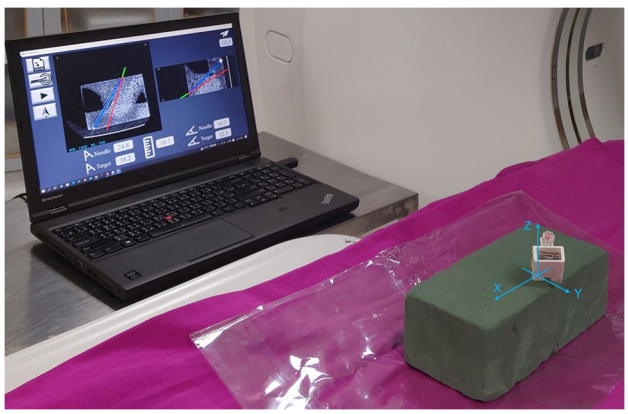

Fig. 5 The photograph showed a wireless IMU-assisted CT-guided needle insertion system. The wet flower mud sponge phantom with embedded target metallic beads in the CT gantry. CT scan DICOM images and IMU orientation were sent to the processing laptop. The operator adjusted the needle angle according to the display on the laptop monitor and made it well-aligned with desired needle trajectory

Success was defined as the needle tip reaching the target. The endpoints included the mediolateral angle error of the first pass, caudocranial angle error of the first pass, procedure time, the total number of needle passes, and the total radiation dose. The procedure time was defined as the time interval between the initial needle puncture and the final set of CT imaging. The study was completed using a 64-slice CT scanner (Optima 660, General Electric) with a slice thickness of 1.25 mm. Using the freehand method, the operator advances the needle based on the operator's visuospatial abilities and experience. The laser protractor–assisted method used a homemade laser protractor (Fig. 6). The projected laser line was used as a reference to guide needle angle selection, and the laser light was kept on the hub of the needle throughout advancement.

Statistical analysis

Data were summarized using descriptive statistics (mean ± SD for continuous variables). Data were analyzed using Kruskal–Wallis H and Dunn's post hoc analysis. A p-value of ≤ 0.05 was set to indicate statistical significance. SPSS system (IBM SPSS Statistics, Version 22.0) was used for statistical analysis.

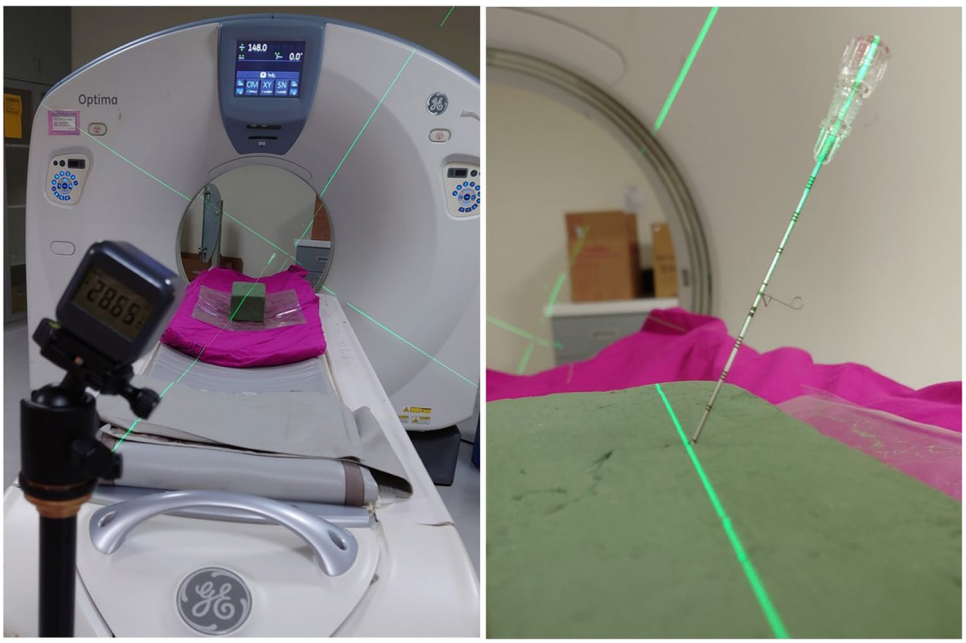

Fig. 6 A homemade laser protractor was used in our hospital to assist CT-guided procedures. The projected green laser line could be used as a reference to guide needle angle selection

Results

The performance of three operators with 8, 2, and 0 years of experience using three CT-guided needle insertion methods (IMU-assisted, laser protractor–assisted, and freehand methods) for target group A (mediolateral angles > 30 degrees), target group B (caudocranial angles > 30 degrees) and target group C (caudocranial angles > 30 degrees, mediolateral angles > 30 degrees) is listed in Table 2. There was no significant difference in the number of needle passes, procedure time, and mediolateral or caudocranial angle error of the first pass using the IMU-assisted method between the three operators. By laser protractor–assisted method, the experienced operator showed lesser mediolateral angle error of the first pass ($p = 0.031$). By the freehand method, the experienced operator showed fewer needle passes ($p = 0.038$) and a reduced procedure time ($p = 0.06$).

Table 2 The performance of three operators using three CT-guided needle insertion methods

Experience of the operator	8 years	2 years	0 year	*p* value
IMU-assisted				
Number of the needle pass	1.1 ± 0.3	1.2 ± 0.4	1.2 ± 0.6	0.582
Procedure time (min)	2.9 ± 1.2	3.0 ± 0.7	3.1 ± 1.6	0.392
Mediolateral angle error of the first pass (°)	1.1 ± 1.2	1.6 ± 1.1	1.6 ± 1.2	0.223
Caudocranial angle error of the first pass (°)	1.3 ± 1.5	1.3 ± 1.3	1.0 ± 0.6	0.931
Radiation dose (mGy-cm)	244.7 ± 66.3	254.2 ± 91.9	252.6 ± 65.9	0.994
Laser protractor–assisted				
Number of the needle pass	2.4 ± 1.8	3.1 ± 1.3	3.3 ± 1.7	0.110
Procedure time (min)	5.0 ± 2.2	7.2 ± 2.7	9.0 ± 3.4	0.055
Mediolateral angle error of the first pass (°)	1.0 ± 0.8	1.5 ± 1.1	2.3 ± 1.5	0.031
Caudocranial angle error of the first pass (°)	3.7 ± 3.3	6.4 ± 6.3	5.8 ± 4.0	0.268
Radiation dose (mGy-cm)	424.2 ± 250.9	491.9 ± 251.8	537.6 ± 282.0	0.460
Freehand				
Number of the needle pass	2.7 ± 1.5	3.6 ± 1.5	4.5 ± 2.5	0.038
Procedure time (min)	5.0 ± 2.6	6.0 ± 2.3	7.6 ± 3.7	0.060
Mediolateral angle error of the first pass (°)	3.9 ± 2.4	2.9 ± 1.8	4.2 ± 3.1	0.463
Caudocranial angle error of the first pass (°)	2.9 ± 1.5	4.7 ± 3.4	4.1 ± 3.7	0.551
Radiation dose (mGy-cm)	446.4 ± 271.2	547.1 ± 308.0	690.7 ± 402.7	0.169

Date are means ± standard deviations

The performance of three CT-guided needle insertion methods is listed in Table 3. There was a significant difference in the number of needle passes (IMU 1.2 ± 0.42, laser protractor 2.9 ± 1.6, freehand 3.6 ± 2.0 time, $p < 0.001$), procedure time (IMU 3.0 ± 1.2, laser protractor 6.4 ± 2.9, freehand 6.2 ± 3.1 min, $p < 0.001$), mediolateral angle error of the first pass (IMU 1.4 ± 1.2, laser protractor 1.6 ± 1.3, freehand 3.7 ± 2.5 (°), $p < 0.001$), caudocranial angle error of the first pass (IMU 1.2 ± 1.2, laser protractor 5.3 ± 4.7, freehand 3.9 ± 3.1 (°), $p < 0.001$), radiation dose (IMU 250.5 ± 74.1, laser protractor 484.6 ± 260.2, freehand 561.4 ± 339.8 (mGy-cm), $p < 0.001$) among three CT-guided needle insertion methods. The subsequent post hoc pairwise comparisons showed that the IMU-assisted method had a significant decrease in the number of needle passes: IMU vs. laser protractor ($p < 0.001$) and IMU vs. freehand ($p < 0.001$). The IMU-assisted method showed a significant decrease in procedure time: IMU vs. laser protractor ($p < 0.001$) and IMU vs. freehand ($p < 0.001$). IMU-assisted and laser protractor–assisted methods showed a significant decrease in mediolateral angle error of the first pass: IMU vs. freehand ($p < 0.001$) and laser protractor vs. freehand ($p < 0.001$). The IMU-assisted method showed a significant decrease in caudocranial angle error of the first pass: IMU vs. laser protractor ($p < 0.001$) and IMU vs. freehand ($p < 0.001$). The IMU-assisted method showed a significant decrease in radiation dose: IMU vs. laser protractor ($p < 0.001$), and IMU vs. freehand ($p < 0.001$).

Discussion

Accuracy of needle placement is paramount for the success of thermal ablation or percutaneous biopsy. We developed a wireless IMU-assisted CT-guided needle insertion system to facilitate needle angle and depth navigation during percutaneous CT-guided procedures. Our results suggest that the IMU-assisted system improves the accuracy of needle insertion compared to the conventional freehand method and laser protractor–guided method. In addition, there is a significant decrease in the number of needle passes, procedure time, mediolateral angle error of the first pass, caudocranial angle error of the first pass, and radiation dose using IMU-assisted methods.

By the IMU method, the performance among the three operators showed no significant difference. Thus, wireless

Table 3 The performance of three CT-guided needle insertion methods

CT-guided methods	IMU	Laser protractor	Freehand	*p* value
Number of the needle pass	1.2 ± 0.42	2.9 ± 1.6	3.6 ± 2.0	< 0.001
Pairwise comparison				
IMU vs laser protractor				< 0.001
IMU vs freehand				< 0.001
Laser protractor vs freehand				0.514
Procedure time (min)	3.0 ± 1.2	6.4 ± 2.9	6.2 ± 3.1	< 0.001
Pairwise comparison				
IMU vs laser protractor				< 0.001
IMU vs freehand				< 0.001
Laser protractor vs freehand				1
Mediolateral angle error of the first pass (°)	1.4 ± 1.2	1.6 ± 1.3	3.7 ± 2.5	< 0.001
Pairwise comparison				
IMU vs laser protractor				1
IMU vs freehand				< 0.001
Laser protractor vs freehand				< 0.001
Caudocranial angle error of the first pass (°)	1.2 ± 1.2	5.3 ± 4.7	3.9 ± 3.1	< 0.001
Pairwise comparison				
IMU vs laser protractor				< 0.001
IMU vs freehand				< 0.001
Laser protractor vs freehand				0.966
Radiation dose (mGy-cm)	250.5 ± 74.1	484.6 ± 260.2	561.4 ± 339.8	< 0.001
Pairwise comparison				
IMU vs laser protractor				< 0.001
IMU vs freehand				< 0.001
Laser protractor vs freehand				1

Date are means ± standard deviations

IMU is very user-friendly. Using the laser protractor–assisted method, the experienced operator exhibits lesser mediolateral angle error on the first pass, which may be explained by the fact that the experienced operator was more familiar with laser protractor usage. Using the freehand method, the experienced operators show a significantly decreased number of needle passes and a reduced procedure time due to a better visuospatial ability to adjust the needle angle.

Compared to electromagnetic (EM) navigation or optical tracking method, our method is simpler in its setup and has a shorter setup time. Using both EM and optical tracking methods requires an additional 15–60 min for fiducial placement, co-registration, and trajectory planning [4]. On the contrary, IMU preparation requires 5–10 min by positioning the IMU on the flat CT table, turning it on, calibrating, and arranging the vehicle-mounted needle. In our design, the IMU can be reused, and there is no additional disposable expense to the procedure. Commercially manufactured vehicles in a single-use or disposable form may be adopted in the future, providing safer, time-saving solutions for users. The limitations of EM tracking include that the magnetic field created by the field generator can be impeded by an external magnetic field, which currently limits its application with MR guidance [1, 17] and is relatively contraindicated in patients with cardiac implantable devices [18]. The optical-based systems require a direct line of view between the cameras and the fiducials located on the instrument and the patient's skin, thus limiting their application in clinical practice. Compared with the laser protractor–assisted method, both craniocaudal and mediolateral angles can be measured simultaneously. Thus, the craniocaudal angle offset during the puncture is minimized. In the freehand method, the operator tends to choose needle trajectory with minimal craniocaudal angle; however, in certain situations, such as a liver dome or subpleural location, a larger craniocaudal angle is mandatory to avoid traversing aerated lung or ribs. In this situation, a navigation system is beneficial.

The gyroscope is used in both IMU-guided and smartphone-guided CT-guided needle insertion. The limitation of applying a gyroscope in a percutaneous CT-guided procedure is that the baseline drifts over time. It is acceptable if the procedure takes at most half an hour. The advantage of using the IMU over smartphones includes a short restart calibration time and needle-holding stability. In the IMU-assisted method, the operator can focus on the laptop monitor and does not need to hold a smartphone during the procedure. The axial and reformed sagittal views on the laptop monitor provide straightforward information on both mediolateral and craniocaudal angles for planned trajectories and inserted needles, and it is beneficial during double oblique needle puncture. The laser-assisted method requires a C-arm cone-beam CT, which increases ionizing radiation exposure and is unavailable in every institution due to expense. Routinely applying this expansive equipment in a CT-guided procedure is time-consuming and less cost-effective.

Potential navigational inaccuracies may arise from needle banding and errors from the 3D-printed vehicle. The limitations of the IMU-assisted CT-guided needle insertion system are as follows: First, it cannot compensate for elastic organ deformations (such as deformation of the tissue during needle advancement or deformation of the lung and liver during respiration). Second, it lacks real-time imaging. Thus, respiratory motion can make precise targeting difficult and may require respiratory reference tracking. In the future study, a system that ensembles a respiratory-gated system and an IMU could be developed, which would be advantageous in real-world practice. Besides, the depths of our target lesions ranged from 8 to 13 cm, which was limited by the length of the coaxial needle and the size of our phantom. However, these depths are reasonable approximations of clinical cases.

The wireless IMU improves accuracy and decreases the procedure time in CT-guided punctures. Thus, the risk to the patient can be minimized. This can reduce needle misplacement and repeated puncture attempts and helps to achieve a predictable and reproducible result without heavy reliance on the interventionalist's experience.

Conclusion

In conclusion, our results show that the wireless IMU improves the angle accuracy and speed of CT-guided needle punctures as compared with laser protractor guidance and freehand technique. The puncture can be performed more accurately and quickly with fewer images, thus minimizing the radiation dose during the procedure.

Funding This work was supported by the National Cheng Kung University Hospital of Taiwan (NCKUH-11201007 and NCKUH-11203049) and the Ministry of Science and Technology of Taiwan (MOST 111-2314-B-006-106).

Declarations

Guarantor The scientific guarantor of this publication is Chao-Chun Chang.

Conflict of interest The authors of this manuscript declare no relationships with any companies, whose products or services may be related to the subject matter of the article.

Statistics and biometry No complex statistical methods were necessary for this paper.

Informed consent Written informed consent was not required for this study because our study is a phantom study.

Ethical approval Institutional Review Board approval was not required because our study is a phantom study.

Methodology
- prospective
- experimental
- performed at one institution

References

1. Chehab MA, Brinjikji W, Copelan A, Venkatesan AM (2015) Navigational tools for interventional radiology and interventional oncology applications. Semin Intervent Radiol 32:416–427
2. Gruber-Rouh T, Schulz B, Eichler K, Naguib ruber-Rou NN, Vogl TJ, Zangos S (2015) Radiation dose and quickness of needle CT-interventions using a laser navigation system (LNS) compared with conventional method. Eur J Radiol 84:1976–1980
3. Komaki T, Hiraki T, Kamegawa T et al (2020) Robotic CT-guided out-of-plane needle insertion: comparison of angle accuracy with manual insertion in phantom and measurement of distance accuracy in animals. Eur Radiol 30:1342–1349
4. Sanchez Y, Anvari A, Samir AE et al (2017) Navigational guidance and ablation planning tools for interventional radiology. Curr Probl Diagn Radiol 46:225–233
5. Bale R, Widmann G (2007) Navigated CT-guided interventions. Minim Invasive Ther Allied Technol 16:196–204
6. Kloeckner R, dos Santos DP, Schneider J et al (2013) Radiation exposure in CT-guided interventions. Eur J Radiol 82:2253–2257
7. Ringe KI, Pohler GH, Rabeh H et al (2021) Electromagnetic navigation system-guided microwave ablation of hepatic tumors: a matched cohort study. Cardiovasc Intervent Radiol 44:500–506
8. Schubert T, Jacob AL, Pansini M et al (2013) CT-guided interventions using a free-hand, optical tracking system: initial clinical experience. Cardiovasc Intervent Radiol 36:1055–1062
9. Chan JWY, Yu PSY, Lau RWH et al (2020) ARTIS Pheno ((R)) the future of thoracic hybrid theatre for lung nodule resection? J Thorac Dis 12:4602–4605
10. Cheng YF, Chen HC, Ke PC et al (2020) Image-guided video-assisted thoracoscopic surgery with Artis Pheno for pulmonary nodule resection. J Thorac Dis 12:1342–1349
11. Xu S, Krishnasamy V, Levy E et al (2018) Smartphone-guided needle angle selection during CT-guided procedures. AJR Am J Roentgenol 210:207–213
12. Weizman Y, Tirosh O, Fuss FK, Tan AM, Rutz E (2022) Recent state of wearable IMU sensors use in people living with spasticity: a systematic review. Sensors (Basel) 22(5):1791
13. Ali SM, Arjunan SP, Peters J et al (2022) Wearable sensors during drawing tasks to measure the severity of essential tremor. Sci Rep 12:5242
14. Natarajan P, Fonseka RD, Sy LW, Maharaj MM, Mobbs RJ (2022) Analysing gait patterns in degenerative lumbar spine disease using inertial wearable sensors - an observational study. World Neurosurg 163:e501–e515
15. Jost GF, Walti J, Mariani L et al (2017) Inertial measurement unit-assisted implantation of thoracic, lumbar, and sacral pedicle screws improves precision of a freehand technique. World Neurosurg 103:11–18
16. Jost GF, Walti J, Mariani L et al (2019) Inertial measurement unit-assisted implantation of pedicle screws in combination with an intraoperative 3-dimensional/2-dimensional visualization of the spine. Oper Neurosurg (Hagerstown) 16:326–334
17. M Lanouziere, O Varbedian, O Chevallier, et al Computed tomography-navigation electromagnetic system compared to conventional computed tomography guidance for percutaneous lung biopsy: a single-center experience. Diagnostics (Basel) 11 (2021)
18. Ernst A, Silvestri GA, Johnstone D et al (2003) Interventional pulmonary procedures: guidelines from the American College of Chest Physicians. Chest 123:1693–1717